FEBS Letters 588 (2014) 52–57

journal homepage: www.FEBSLetters.org

An N-terminal pro-atrial natriuretic peptide (NT-proANP) 'aggregation-prone' segment involved in isolated atrial amyloidosis

Nikolaos N. Louros [a], Vassiliki A. Iconomidou [a], Paraskevi L. Tsiolaki [a], Evangelia D. Chrysina [b], Georgios E. Baltatzis [c], Efstratios S. Patsouris [c], Stavros J. Hamodrakas [a,*]

[a] Department of Cell Biology and Biophysics, Faculty of Biology, University of Athens, Panepistimiopolis, Athens 157 01, Greece
[b] Institute of Biology, Medicinal Chemistry and Biotechnology, National Hellenic Research Foundation, 48 Vassileos Constantinou Avenue, Athens 116 35, Greece
[c] 1st Department of Pathology, Medical School, University of Athens, 75 Mikras Assias, Goudi 115 27, Greece

ARTICLE INFO

Article history:
Received 3 September 2013
Revised 8 October 2013
Accepted 30 October 2013
Available online 9 November 2013

Edited by Jesus Avila

Keywords:
Natriuretic peptide
N-terminal pro-atrial natriuretic peptide (NT-proANP)
Amyloid fibril
Isolated atrial amyloidosis (IAA)
Cardiac amyloidose

ABSTRACT

Isolated atrial amyloidosis (IAA) is a common localized form of amyloid deposition within the atria of the aging heart. The main constituents of amyloid fibrils are atrial natriuretic peptide (ANP) and the N-terminal part of its precursor form (NT-proANP). An 'aggregation-prone' heptapeptide (^{114}KLRALLT^{120}) was located within the NT-proANP sequence. This peptide self-assembles into amyloid-like fibrils in vitro, as electron microscopy, X-ray fiber diffraction, ATR FT-IR spectroscopy and Congo red staining studies reveal. Consequently, remedies/drugs designed to inhibit the aggregation tendency of this 'aggregation-prone' segment of NT-proANP may assist in prevention/treatment of IAA, congestive heart failure (CHF) or atrial fibrillation (AF).

1. Introduction

Several soluble proteins and peptides have the ability to aggregate under certain conditions into higher-order fibrillar structures known as amyloid fibrils [1,2]. Deposition of amyloid fibrils in various tissues and organs has been associated with a variety of pathological conditions termed amyloidoses [3]. This diverse group of conformational diseases includes, amongst others, a number of neurodegenerative disorders (such as Alzheimer's, Parkinson's and Huntington's), prion diseases, type II diabetes, several cases of carcinomas (e.g. medullary carcinoma, prolactinoma or insulinoma), heart conditions (cardiac amyloidoses), etc. [4].

Amyloid deposition in the elderly heart is an ordinary finding [5]. Cardiac amyloidosis is divided into two distinct types, a systemic and a localized form. The first type, designated as senile systemic amyloidosis (SSA), is associated with the formation of amyloid fibrils, derived from transthyretin (TTR), mainly in the cardiac ventricles [6]. The second type, called isolated atrial amyloidosis (IAA), involves the localized deposition of amyloid fibrils in the atria of the aging heart [7]. As an age related condition, it frequently appears after the fourth decade and prevails in higher age groups (>80–85% in ages above 80 years) [8], showing a predisposition for females [9]. Experimental evidence and clinical studies have indicated an increased frequency associated with different cardiac diseases, such as congestive heart failure (CHF), atrial fibrillation (AF) and atrial thromboembolism [10,11]. Additional clinical effects of amyloid deposits in the heart atria involve, apart from cardiac failure, several rhythm disturbances [12], deriving from damaged diastolic function due to the mechanical disturbance of myocyte movement by the diffuse deposition of amyloid [13].

Atrial natriuretic peptide (ANP) has been identified as the primary component of IAA amyloid fibrils [14]. However, immunohistochemical studies have also signified the presence of the N-terminal remnant of its precursor form, $^{1-98}$proANP and Brain Natriuretic Peptide (BNP) [14,15]. It is expressed and stored in cytoplasmic granules of the myocyte cells of the cardiac atria. The major stimulant for ANP release is atrial wall stretch as an after-effect of increased intravascular volume [16]. The human pre-proANP precursor, containing a hydrophobic signal peptide (residues 1–25), is cleaved to form the 126 amino acid long proANP precursor (Fig. 1). ProANP undergoes further cleavage by a specific

Abbreviations: NT-proANP, N-terminal pro-atrial natriuretic peptide; ANP, atrial natriuretic peptide; BNP, brain natriuretic peptide; IAA, isolated atrial amyloidosis; SSA, senile systemic amyloidosis; TTR, transthyretin; CHF, congestive heart failure; AF, atrial fibrosis; cGMP, cyclic guanosine monophosphate; ATR FT-IR spectroscopy, attenuated total reflectance Fourier-transform spectroscopy

* Corresponding author. Fax: +30 210 7274254.
E-mail address: shamodr@biol.uoa.gr (S.J. Hamodrakas).

0014-5793/$36.00
http://dx.doi.org/10.1016/j.febslet.2013.10.049

cardiac serine protease called corin, immediately after secretion, resulting in the production of the final mature $^{1-28}$ANP product, a 28 amino acid long hormone and the N-terminal remnant $^{1-98}$pro-ANP (hereinafter called NT-proANP) [17].

The exact biological role of ANP still remains unclear. After secretion in the plasma, ANP contributes in the control of circulating blood volume [18]. Moreover, it binds to guanylyl-cyclase ANP-receptors, located in various organs, such as the brain, blood vessels, kidney and adrenal glands, activating cGMP cascade pathways [19]. ANP is rapidly cleared from the blood stream by binding to type C ANP receptors and neutral endopeptidases, both located in the kidney and blood vessels [20]. NT-proANP has a longer half-life than ANP [21] and even though its exact biological function is not determined yet, it has been suggested as a biological marker for left ventricular dysfunction [22].

Detailed theoretical and experimental evidence has repeatedly indicated that amyloid formation is mediated by specific short sequence regions/stretches of a polypeptide chain that have a higher aggregation propensity and therefore vitally contribute to its aggregation tendency [23,24]. In this work, we determine a novel aggregation-potent segment of NT-proANP, ^{114}KLRALLT^{120}, which was initially predicted as such, by implementing AMYLPRED, our aggregation propensity algorithm [25]. This aggregation-prone peptide segment was synthesized (see Section 2) and here we present experimental results, verifying its strong aggregation propensity to form amyloid fibrils. It should be mentioned at this point that, a distantly homologous peptide, KMVLYTL, has also been determined to possess a strong aggregation propensity in the sequence of the N-terminal pro-brain natriuretic peptide (NT-proBNP) [26]. An analysis of the physico-chemical properties of both peptides is provided (see Supplementary Table 1 and Fig. S1) [27]. Also, we discuss our findings, implicating NT-proANP as one of the main the driving forces in IAA fibril formation, providing a novel target for IAA prevention/prohibition.

2. Materials and methods

2.1. Prediction of potential aggregation prone peptides in NT-proANP and peptide synthesis

Our prediction algorithm AMYLPRED, a consensus prediction tool of potential 'aggregation-prone' peptides (freely accessible to academic users at http://biophysics.biol.uoa.gr/AMYLPRED) [25], was implemented on the amino acid sequence of the $^{1-151}$ANP pre-pro-hormone. As a result, a segment of NT-proANP, with high aggregation propensity was predicted (see Fig. 1). This heptapeptide, KLRALLT (nominal positions 114–120), is located close to the C-terminal region of NT-proANP (Fig. 1). The NT-proANP heptapeptide-analogue KLRALLT was synthesized by GeneCust Europe, Luxembourg (purity >98%, free N- and C-terminals).

2.2. Formation of amyloid-like fibrils

The synthesized NT-proANP heptapeptide-analogue, KLRALLT, was dissolved in distilled water (pH 5.75), at a concentration of 15 mg ml^{-1}. After an incubation period of 1–2 weeks, mature amyloid-like fibril containing gels were formed. However production of oriented fibers, suitable for X-ray diffraction, were obtained from solutions of higher concentration of the peptide, containing mature amyloid-like fibrils as described below.

2.3. X-ray fiber diffraction

The NT-proANP heptapeptide-analogue, KLRALLT, was dissolved in distilled water (pH 5.75) at a concentration of 20 mg ml^{-1} to produce mature amyloid-like fibrils, after 1–2 weeks incubation, forming a fibril-containing gel. A droplet (10 μl) of the fibril containing solution was placed between two aligned siliconized glass rods (spaced 2 mm apart). The droplet was allowed to dry slowly at ambient temperatures and humidities, for 1 h, to form an oriented fiber suitable for X-ray diffraction. The X-ray diffraction pattern was collected, using a SuperNova-Agilent Technologies X-ray generator equipped with a 135-mm ATLAS CCD detector and a 4-circle kappa goniometer, at the Institute of Biology, Medicinal Chemistry and Biotechnology, National Hellenic Research Foundation (CuK_α high intensity X-ray micro-focus source, $\lambda = 1.5418$ Å), operated at 50 kV, 0.8 mA. The specimen-to-film distance was set at 117 mm and the exposure time was set to 180s. The X-ray pattern, initially viewed using the program CrysAlisPro [28] was displayed and measured with the aid of the program iMosFLM [29].

2.4. Congo red staining and polarized light microscopy

Fibril suspensions of the peptide solution were applied to glass slides and were air-dried at ambient temperatures and humidities. The film produced, containing amyloid-like fibrils, was stained

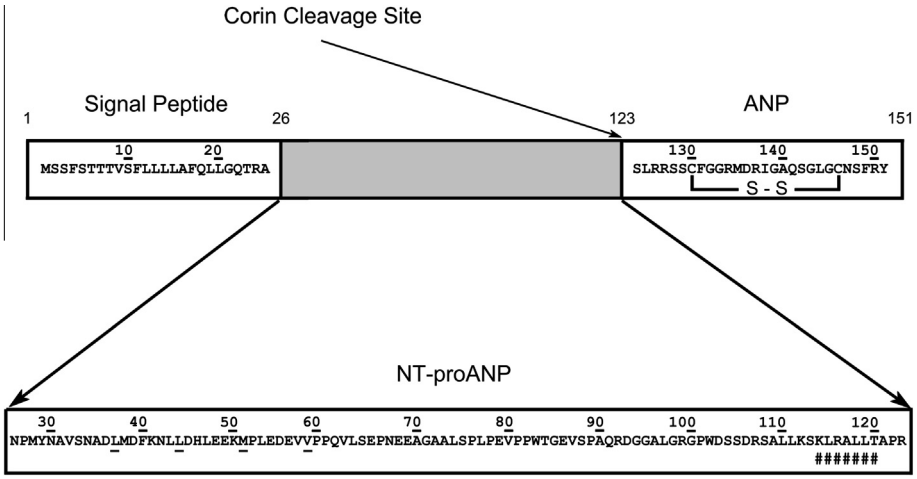

Fig. 1. The amino acid composition of full length atrial natriuretic peptide. It is expressed as a 151 amino acid long pre-pro-hormone, in the atrial myocyte cells. The prohormone form, composed of 126 amino acids, is produced after cleavage of the signal peptide and it is the predominant form stored within the atrial granules. Cleavage by a corin enzyme immediately after secretion results in the 28 amino acids in length mature ANP and the N-terminal remnant, known as NT-proANP. The predicted 'aggregation-prone' region of NT-proANP is marked with "#" under the sequence. The four underlined hydrophobic residues located at the N-terminal segment of NT-proANP (nominal residues 37–59), show heptad periodicities of hydrophobic residues, a coiled–coil motif (a motif capable of forming a superhelix of α-helices) [26,47].

with a 1% Congo red solution in distilled water (pH 5.75) for 20 min [30]. Excess stain was removed through tap water washes [30]. The samples were observed under bright field illumination and between crossed polars, using a Leica MZ75 polarizing stereomicroscope equipped with a JVC GC-X3E camera.

2.5. Negative staining

For negative staining, a drop (~5 μl) of the fibril containing solutions of the KLRALLT peptide was applied to glow-discharged 400-mesh carbon-coated copper grids, for 60 s. The grids were flash-washed with distilled water and stained with a drop of 2% (w/v) aqueous uranyl acetate for 60 s. Excess stain was removed by blotting with a filter paper. The fibril containing grids were initially air-dried and examined with a Morgagni™ 268 transmission electron microscope, operated at 80 kV. Digital acquisitions were performed with an 11 Mpixel side-mounted Morada CCD camera (Soft Imaging System, Muenster, Germany).

2.6. Attenuated total reflectance Fourier-transform infrared spectroscopy and post-run spectra computations

A 10-μl drop of the fibril containing solution of the NT-proANP heptapeptide-analogue was cast on a front-coated Au mirror and left to dry slowly at ambient conditions to form a thin film. IR spectra were obtained at a resolution of 4 cm^{-1}, utilizing an IR microscope (IRScope II, BrukerOPTICS, Bruker Optik GmbH, Ettlingen, Germany), equipped with a Ge ATR objective lens (20×) and attached to a FT-IR spectrometer (Equinox 55, BrukerOPTICS). Ten 32-scan spectra were collected from each sample and averaged to improve the *S*/*N* ratio. All spectra are shown in the absorption mode, after correction for the wavelength-dependence of the penetration depth (d_p analogous λ). Derivatives were computed analytically using routines of the Bruker OPUS/OS2 software including smoothing over a ±8 cm^{-1} range around each data point, performed by the Savitsky–Golay algorithm [31]. Smoothing over narrower ranges resulted in deterioration of the *S*/*N* ratio and did not increase the number of minima that could be determined with confidence. The minima in the second derivative were used to determine the corresponding absorbtion band maxima.

3. Results

After incubation for 1–2 weeks, the KLRALLT peptide self-assembles into amyloid-like fibrils (Fig. 2a and b), forming gels. Electron micrographs display the amyloid-like fibrils to be straight and unbranched with an indefinite length (several microns long) and a diameter of approximately 50–60 Å (Fig. 2a). Frequently, the fibrils coalesce laterally and in register forming ribbons, varying in diameter (Fig. 2b). This apparent morphological polymorphism has previously been established as a common characteristic of amyloid-like fibrils formed by several aggregation-prone peptides or proteins [32]. Furthermore, the presence of supramolecular spherical structures (Fig. 2a, arrows) signifies the possibility that the KLRALLT peptide self-assembles, initially forming spherulites. Spherulites have been associated with early amyloid fibrillogenesis events, for several proteins involved in the formation of functional [33] or pathological amyloids, as possible pre-fibrillar amyloid intermediates and are implicated with the cytotoxicity mechanisms of amyloidoses [34,35].

The X-ray diffraction pattern produced by an oriented fiber, formed by solutions containing amyloid-like fibrils from the peptide KLRALLT, resembles a typical "cross-β" architecture that amyloid fibrils adopt (Fig. 3) [36,37]. Specifically, a strong reflection at 4.7 Å is attributed to the interchain distance between hydrogen bonded β-strands. Furthermore, the spacing at 11.9 Å is ascribed to the packing distance between packed β-sheets. However, there is no preferential orientation of these two reflections along the meridian or the equator of the X-ray diffraction pattern, as in a typical cross-β pattern, implying that the amyloid-like fibrils adopt all possible orientations in the fiber (which is not really oriented!).

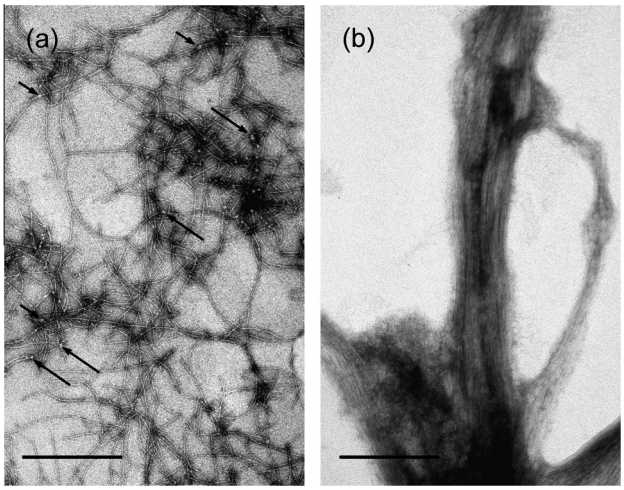

Fig. 2. Electron micrographs of amyloid-like fibrils derived by self-assembly, from a 15 mg ml^{-1} solution of KLRALLT peptide in distilled water (pH 5.75). (a) Amyloid-like fibrils appear straight, unbranched and of undetermined length with a diameter of ca. 50–60 Å. Pre-fibrillar spherical aggregates, called spherulites, are also formed (single arrows) indicating the ability of the KLRALLT peptide to nucleate (bar 500 nm). (b) Amyloid-like fibrils interact in a lateral fashion forming ribbons varying in diameter (bar 500 nm). The fibrillar polymorphism observed has previously been established as a common characteristic of amyloid-like fibrils formed by several aggregation-prone peptides or proteins [32].

Complementary experimental evidence produced by the ATR FT-IR (1500–1800 cm^{-1}) spectrum of the KLRALLT peptide, supports the presence of an antiparallel β-sheet conformation for this peptide, in agreement to the results obtained from X-ray diffraction (Fig. 4). Particularly, the spectrum displays a strong amide I band at 1624 cm^{-1}, due to the preponderance of β-sheet,

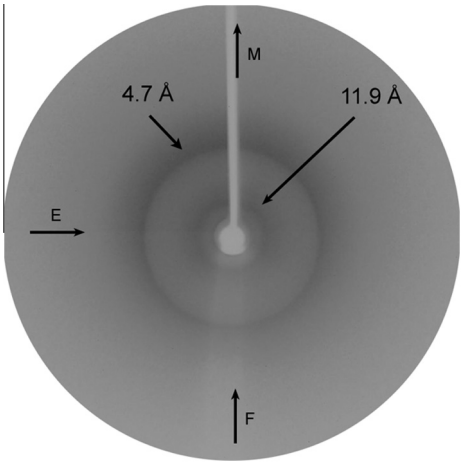

Fig. 3. X-ray diffraction pattern from an 'oriented' fiber of the NT-proANP KLRALLT peptide-analogue amyloid-like fibrils. The fiber axis (*F*) is vertical (meridian, *M*), whereas the equator is horizontal (*E*). The "cross-β" structure is evident. A 4.7 Å reflection is due to the distance between successive hydrogen bonded β-strands and a 11.9 Å reflection results from the spacing between packed β-sheets. However, there is no preferential orientation (the reflections appear as rings) of the meridional and equatorial reflections (it is not a typical oriented "cross-β" pattern). See, also Section 3.

supported by the amide II band at 1535 cm^{-1} [38–40]. Moreover, the additional component at 1693 cm^{-1}, in the amide I band, is probably an indication that the β-sheets are antiparallel (Table 1) [38–40]. Proteins containing antiparallel β-sheets usually exhibit a high frequency β-sheet component that arises from transition dipole coupling, typically located 50–70 cm^{-1} higher than the main β-sheet band [40]. The detailed spectrum, in the region 1100–1800 cm^{-1}, is also provided (Supplementary Table 2 and Fig. S2).

Amyloid-like fibrils have been shown to bind the stain Congo red [41]. Films produced by the fibril containing peptide KLRALLT solutions were initially stained by the characteristic for amyloid fibrils Congo red dye (see Section 2) and then were studied under a polarizing microscope. Amyloid deposits composed of KLRALLT amyloid-like fibrils bind Congo red, as observed under bright field illumination (Fig. 5a) and exhibit the characteristic for amyloid fibrils apple/green birefringence when viewed under crossed polars (Fig. 5b).

4. Discussion

Amyloids arise from self-aggregating proteins or peptides with diverse functional properties, different amino acid sequences and structural characteristics. A growing number of such proteins and peptides have been found to form amyloid fibrils, both in vitro and in vivo, supporting early observations, which led to the concept that, every protein may adopt both a globular and a fibrillar structure under appropriate conditions [42]. Several studies, both theoretical and experimental, have shown that self-aggregating proteins contain potent aggregation-prone segments within their native sequence [23,25,43]. Such aggregation-prone peptide regions have been proposed to act as templates for amyloid fibril formation after protein structural rearrangements [25]. An impressive genome-wide survey revealed that most proteins contain at least one peptide region with such a high aggregation tendency [43].

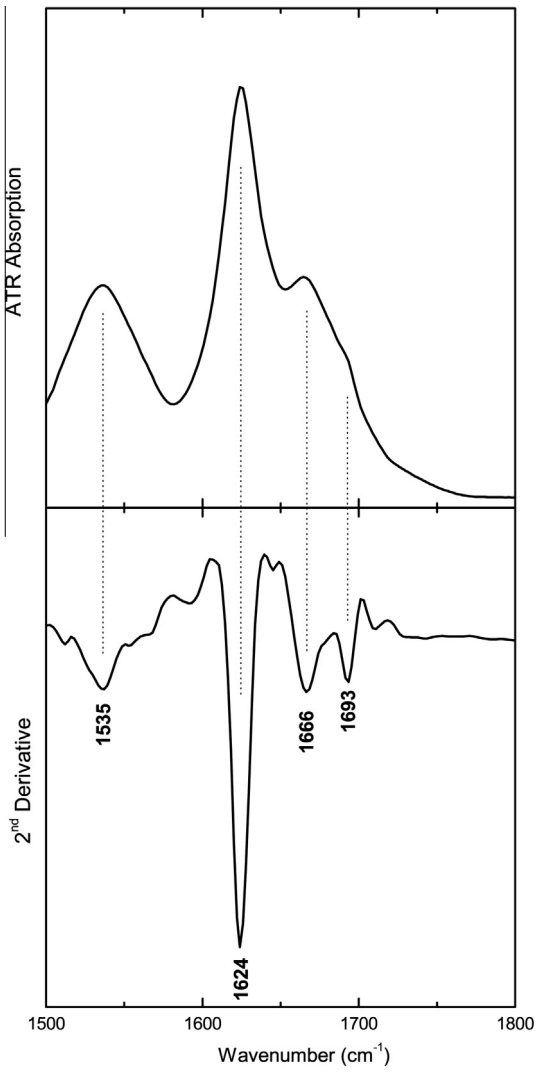

Fig. 4. ATR FT-IR (1500–1800 cm^{-1}) spectrum obtained from a thin hydrated-film containing mature amyloid-like fibrils derived by KLRALLT peptide self-aggregation. The second derivative spectrum was included to identify the exact band maxima and their tentative assignments. The ATR FT-IR spectrum is indicative of the preponderance of an antiparallel β-sheet secondary structure (Table 1).

Table 1
Bands observed in the ATR FT-IR (1500–1800 cm^{-1}) spectrum produced from a hydrated film of the 'aggregation-prone' heptapeptide, KLRALLT, after self-assembly, and their tentative assignments (Fig. 4).

Bands (cm^{-1})	Assignment
1535	β-Sheet (amide II)
1624	β-Sheet (amide I)
1666	TFA
1693	Antiparallel β-sheet

The KLRALLT peptide was predicted as a potential aggregation-prone peptide segment of NT-proANP by the AMYLPRED algorithm [25]. Our experimental results, presented here (see Section 3), indeed verify that this peptide-analogue self-assembles forming amyloid-like fibrils, which satisfy all the basic criteria for amyloids [41]. Apparently, NT-proANP has an inherent ability to form amyloid fibrils, mainly due to the KLRALLT peptide, in support to previous immunohistochemical data indicating its presence in amyloid deposits of heart atria [15]. Several polypeptide hormones have been identified in both mature and precursor states in amyloid fibrils [44]. Our data corroborate this concept adding ANP and NT-proANP as another hormone-prehormone amyloid fibril formation case.

Previous experimental studies have indicated that ANP polymerization into amyloid fibrils is a nucleation dependent process [45,46]. However, mature ANP has a substantially higher aggregation tendency once seeded [10,45,46]. Therefore, it is possible that pre-fibrillar aggregates are actually formed by NT-proANP, driven by the aggregation propensity of the KLRALLT peptide introducing a nucleation effect for ANP polymerization into amyloid fibrils. This may also explain why, although ANP is the predominant component in amyloid fibrils of the atria, NT-proANP is also found as a secondary supporting component [15]. Further, more refined, experimental work is needed to verify this hypothesis.

Elegant theoretical and experimental work by Richards and coworkers, more than a decade ago, indicated the presence of a coiled–coil motif region (a region capable of forming a superhelix of α-helices), close to the N-terminal of NT-proANP (as seen by the underlined hydrophobic residues in Fig. 1), suggesting that NT-proANP oligomerization may occur via these coiled–coil motifs of hydrophobic residues [47]. Therefore, an alternative approach may involve NT-proANP forming early oligomers through coiled–coils and further polymerizing into atrial amyloid fibrillar structures, as a result of the self-aggregation potential of the KLRALLT aggregation prone peptide. A similar process has recently been proposed to occur for the NT-proBNP natriuretic pro-hormone [26].

It is not clarified yet why polypeptide hormones form amyloid fibrils *in vivo*. Abnormal high concentrations of the polypeptide, close to the hormone secretion site, result in the formation of amyloid deposits in most localized amyloidoses conditions [10]. NT-proANP has a significantly longer half-life compared to ANP [21]. Consequently, it is found in correspondingly higher concentrations both in plasma and heart atria. Additionally, ANP and NT-proANP

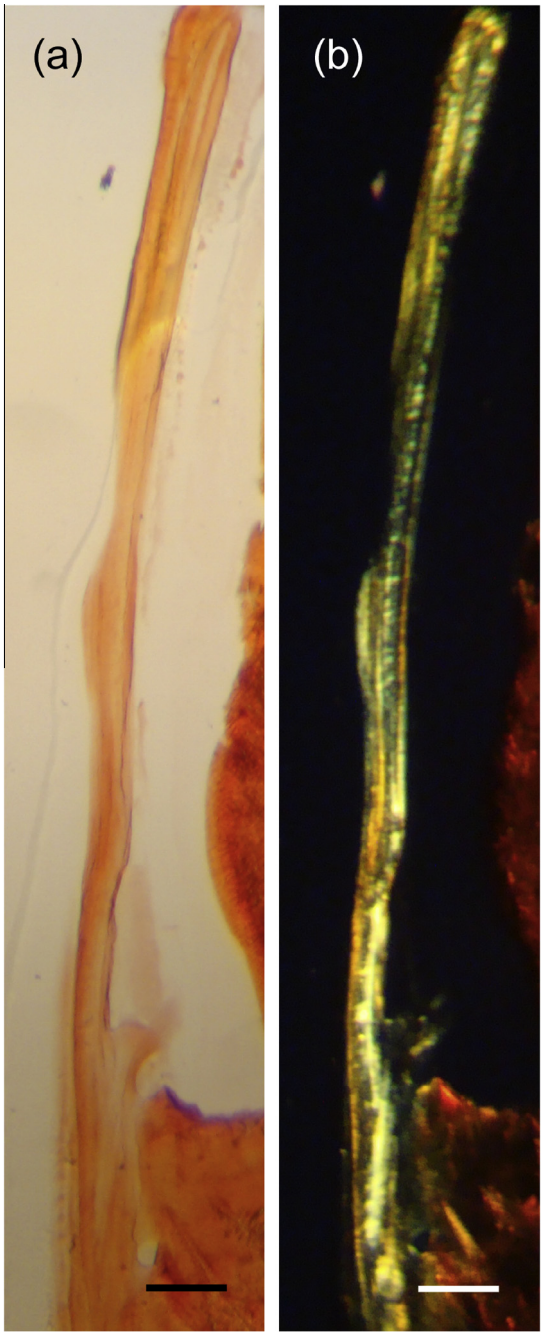

Fig. 5. Photomicrographs of an amyloid-like fibril containing gel, derived from KLRALLT peptide-analogue self-assembly, stained with Congo red. (a) The Congo red dye is bound, as seen under bright field illumination. (b) The apple-green birefringence that amyloids typically exhibit is clearly seen under crossed polars. Bar 100 μm.

secretion is reported higher in patients with heart conditions, such as congestive heart failure or atrial fibrillation [9]. As a result, high concentrations of NT-proANP within the heart atria may promote amyloid deposit formation, leading to IAA. Therefore, NT-proANP aggregation preventing techniques may be mandatory to avoid the aforementioned pathological heart conditions. If indeed ANP polymerization is dependent of NT-proANP nucleation, remedies/drugs designed to prevent aggregation of the KLRALLT peptide, following the example of recent impressive studies [48,49], could prove to be of substantial importance in future IAA treatment or prevention.

Acknowledgements

We thank the University of Athens and the National Hellenic Research Foundation for support. We thank Maria Karamolegou for expert technical assistance and our collaborators Drs. Georgios Chryssikos and Vassilis Gionis from the Theoretical and Physical Chemistry Institute of the National Hellenic Research Foundation for help with the ATR FT-IR experiments. We should also like to thank the editor of this manuscript for properly handling it and the anonymous reviewers for useful and constructive criticism.

Appendix A. Supplementary data

Supplementary data associated with this article can be found, in the online version, at http://dx.doi.org/10.1016/j.febslet.2013.10.049.

References

[1] Dobson, C.M. (2003) Protein folding and misfolding. Nature 426, 884–890.
[2] Chiti, F. and Dobson, C.M. (2009) Amyloid formation by globular proteins under native conditions. Nat. Chem. Biol. 5, 15–22.
[3] Pepys, M.B. (1996) The Oxford Textbook of Medicine, Oxford University Press, Oxford.
[4] Buxbaum, J.N. and Linke, R.P. (2012) A molecular history of the amyloidoses. J. Mol. Biol. 421, 142–159.
[5] McCarthy 3rd, R.E. and Kasper, E.K. (1998) A review of the amyloidoses that infiltrate the heart. Clin. Cardiol. 21, 547–552.
[6] Sletten, K., Westermark, P. and Natvig, J.B. (1980) Senile cardiac amyloid is related to prealbumin. Scand. J. Immunol. 12, 503–506.
[7] Steiner, I. (1987) The prevalence of isolated atrial amyloid. J. Pathol. 153, 395–398.
[8] Kawamura, S., Takahashi, M., Ishihara, T. and Uchino, F. (1995) Incidence and distribution of isolated atrial amyloid: histologic and immunohistochemical studies of 100 aging hearts. Pathol. Int. 45, 335–342.
[9] Goette, A. and Rocken, C. (2004) Atrial amyloidosis and atrial fibrillation: a gender-dependent "arrhythmogenic substrate"? Eur. Heart J. 25, 1185–1186.
[10] Johansson, B. and Westermark, P. (1990) The relation of atrial natriuretic factor to isolated atrial amyloid. Exp. Mol. Pathol. 52, 266–278.
[11] van den Berg, M.P., Tjeerdsma, G., Jan de Kam, P., Boomsma, F., Crijns, H.J. and van Veldhuisen, D.J. (2002) Longstanding atrial fibrillation causes depletion of atrial natriuretic peptide in patients with advanced congestive heart failure. Eur. J. Heart Fail. 4, 255–262.
[12] Maredia, N. and Ray, S.G. (2005) Cardiac amyloidosis. Clin. Med. 5, 504–509.
[13] Takemura, G. et al. (1998) Expression of atrial and brain natriuretic peptides and their genes in hearts of patients with cardiac amyloidosis. J. Am. Coll. Cardiol. 31, 754–765.
[14] Linke, R.P., Voigt, C., Storkel, F.S. and Eulitz, M. (1988) N-terminal amino acid sequence analysis indicates that isolated atrial amyloid is derived from atrial natriuretic peptide. Virchows Arch. B 55, 125–127.
[15] Pucci, A., Wharton, J., Arbustini, E., Grasso, M., Diegoli, M., Needleman, P., Vigano, M. and Polak, J.M. (1991) Atrial amyloid deposits in the failing human heart display both atrial and brain natriuretic peptide-like immunoreactivity. J. Pathol. 165, 235–241.
[16] Edwards, B.S., Zimmerman, R.S., Schwab, T.R., Heublein, D.M. and Burnett Jr., J.C. (1988) Atrial stretch, not pressure, is the principal determinant controlling the acute release of atrial natriuretic factor. Circ. Res. 62, 191–195.
[17] Yan, W., Wu, F., Morser, J. and Wu, Q. (2000) Corin, a transmembrane cardiac serine protease, acts as a pro-atrial natriuretic peptide-converting enzyme. Proc. Natl. Acad. Sci. USA 97, 8525–8529.
[18] Levin, E.R., Gardner, D.G. and Samson, W.K. (1998) Natriuretic peptides. N. Engl. J. Med. 339, 321–328.
[19] Waldman, S.A., Rapoport, R.M. and Murad, F. (1984) Atrial natriuretic factor selectively activates particulate guanylate cyclase and elevates cyclic GMP in rat tissues. J. Biol. Chem. 259, 14332–14334.
[20] van den Berg, M.P., van Gelder, I.C. and van Veldhuisen, D.J. (2004) Depletion of atrial natriuretic peptide during longstanding atrial fibrillation. Europace 6, 433–437.
[21] Yandle, T.G., Richards, A.M., Nicholls, M.G., Cuneo, R., Espiner, E.A. and Livesey, J.H. (1986) Metabolic clearance rate and plasma half life of alpha-human atrial natriuretic peptide in man. Life Sci. 38, 1827–1833.
[22] Lerman, A., Gibbons, R.J., Rodeheffer, R.J., Bailey, K.R., McKinley, L.J., Heublein, D.M. and Burnett Jr., J.C. (1993) Circulating N-terminal atrial natriuretic peptide as a marker for symptomless left-ventricular dysfunction. Lancet 341, 1105–1109.
[23] Lopez de la Paz, M. and Serrano, L. (2004) Sequence determinants of amyloid fibril formation. Proc. Natl. Acad. Sci. USA 101, 87–92.
[24] Teng, P.K. and Eisenberg, D. (2009) Short protein segments can drive a non-fibrillizing protein into the amyloid state. Protein Eng. Des. Sel. 22, 531–536.

[25] Frousios, K.K., Iconomidou, V.A., Karletidi, C.M. and Hamodrakas, S.J. (2009) Amyloidogenic determinants are usually not buried. BMC Struct. Biol. 9, 44.
[26] Iconomidou, V.A., Pheida, D., Hamodraka, E.S., Antony, C., Hoenger, A. and Hamodrakas, S.J. (2012) An amyloidogenic determinant in n-terminal pro-brain natriuretic peptide (nt-probnp): implications for cardiac amyloidoses. Biopolymers 98, 67–75.
[27] Gasteiger, E., Hoogland, C., Gattiker, A., Duvaud, S., Wilkins, M.R., Appel, R.D. and Bairoch, A. (2005) Protein identification and analysis tools on the ExPASy server (Walker, M.J., Ed.), The Proteomics Protocols Handbook, pp. 571–607, Humana Press, New York.
[28] Diffraction, Oxford. (2009) Chrysalis Promotions, Oxford Diffraction Ltd., Abingdon, Oxfordshire, England.
[29] Leslie, A.G.W. and Powell, H.R. (2007) Processing diffraction data with mosflm (Read, R. and Sussman, J.L., Eds.), Evolving Methods for Macromolecular Crystallography, ISBN 978-1-4020-6314-5, pp. 41–51, Springer, Dordrecht, The Netherlands.
[30] Romhanyi, G. (1971) Selective differentiation between amyloid and connective tissue structures based on the collagen specific topo-optical staining reaction with Congo red. Virchows Arch. A 354, 209–222.
[31] Savitsky, A. and Golay, M.J.E. (1964) Smoothing and differentiation of data by simplified least-squares procedures. Anal. Chem. 36, 1627–1639.
[32] Kreplak, L. and Aebi, U. (2006) From the polymorphism of amyloid fibrils to their assembly mechanism and cytotoxicity. Adv. Protein Chem. 73, 217–233.
[33] Hamodrakas, S.J., Hoenger, A. and Iconomidou, V.A. (2004) Amyloid fibrillogenesis of silkmoth chorion protein peptide-analogues via a liquid–crystalline intermediate phase. J. Struct. Biol. 145, 226–235.
[34] Moreth, J., Kroker, K.S., Schwanzar, D., Schnack, C., von Arnim, C.A., Hengerer, B., Rosenbrock, H. and Kussmaul, L. (2013) Globular and protofibrillar abeta aggregates impair neurotransmission by different mechanisms. Biochemistry 52, 1466–1476.
[35] Iconomidou, V.A., Leontis, A., Hoenger, A. and Hamodrakas, S.J. (2013) Identification of a novel 'aggregation-prone'/'amyloidogenic determinant' peptide in the sequence of the highly amyloidogenic human calcitonin. FEBS Lett. 587, 569–574.
[36] Geddes, A.J., Parker, K.D., Atkins, E.D. and Beighton, E. (1968) "Cross-beta" conformation in proteins. J. Mol. Biol. 32, 343–358.
[37] Sunde, M., Serpell, L.C., Bartlam, M., Fraser, P.E., Pepys, M.B. and Blake, C.C. (1997) Common core structure of amyloid fibrils by synchrotron X-ray diffraction. J. Mol. Biol. 273, 729–739.
[38] Krimm, S. and Bandekar, J. (1986) Vibrational spectroscopy and conformation of peptides, polypeptides, and proteins. Adv. Protein Chem. 38, 181–364.
[39] Haris, P.I. and Chapman, D. (1995) The conformational analysis of peptides using Fourier transform IR spectroscopy. Biopolymers 37, 251–263.
[40] Jackson, M. and Mantsch, H.H. (1995) The use and misuse of FTIR spectroscopy in the determination of protein structure. Crit. Rev. Biochem. Mol. Biol. 30, 95–120.
[41] Sunde, M. and Blake, C. (1997) The structure of amyloid fibrils by electron microscopy and X-ray diffraction. Adv. Protein Chem. 50, 123–159.
[42] Astbury, W.T., Dickinson, S. and Bailey, K. (1935) The X-ray interpretation of denaturation and the structure of the seed globulins. Biochem. J. 29, 2351–2360.
[43] Goldschmidt, L., Teng, P.K., Riek, R. and Eisenberg, D. (2010) Identifying the amylome, proteins capable of forming amyloid-like fibrils. Proc. Natl. Acad. Sci. USA 107, 3487–3492.
[44] Westermark, P., Wernstedt, C., Wilander, E., Hayden, D.W., O'Brien, T.D. and Johnson, K.H. (1987) Amyloid fibrils in human insulinoma and islets of Langerhans of the diabetic cat are derived from a neuropeptide-like protein also present in normal islet cells. Proc. Natl. Acad. Sci. USA 84, 3881–3885.
[45] Maioli, E., Torricelli, C., Santucci, A. and Pacini, A. (2000) Molecular assembly of endogenous and synthetic big atrial natriuretic peptide (ANP) and its amyloidogenic implications. Biochim. Biophys. Acta 1500, 31–40.
[46] Torricelli, C., Capurro, E., Santucci, A., Paffetti, A., D'Ambrosio, C., Scaloni, A., Maioli, E. and Pacini, A. (2004) Multiple plasma proteins control atrial natriuretic peptide (ANP) aggregation. J. Mol. Endocrinol. 33, 335–341.
[47] Seidler, T., Pemberton, C., Yandle, T., Espiner, E., Nicholls, G. and Richards, M. (1999) The amino terminal regions of proBNP and proANP oligomerise through leucine zipper-like coiled–coil motifs. Biochem. Biophys. Res. Commun. 255, 495–501.
[48] Choi, S., Reixach, N., Connelly, S., Johnson, S.M., Wilson, I.A. and Kelly, J.W. (2010) A substructure combination strategy to create potent and selective transthyretin kinetic stabilizers that prevent amyloidogenesis and cytotoxicity. J. Am. Chem. Soc. 132, 1359–1370.
[49] Connelly, S., Choi, S., Johnson, S.M., Kelly, J.W. and Wilson, I.A. (2010) Structure-based design of kinetic stabilizers that ameliorate the transthyretin amyloidoses. Curr. Opin. Struct. Biol. 20, 54–62.